



Published in final edited form as:

Hepatology. 2016 June ; 63(6): 1900–1913. doi:10.1002/hep.28508.

Differential Requirement for *de novo* Lipogenesis in Cholangiocarcinoma and Hepatocellular Carcinoma of Mice and Humans

Lei Li^{1,2}, Li Che^{2,3}, Kevin M. Tharp⁴, Hyo-Min Park⁴, Maria G. Pilo⁵, Dan Cao^{2,6}, Antonio Cigliano⁷, Gavinella Latte⁵, Zhong Xu^{2,8}, Silvia Ribback⁷, Frank Dombrowski⁷, Matthias Evert^{7,*}, Gregory J. Gores⁹, Andreas Stahl⁴, Diego F. Calvisi⁵, and Xin Chen²

¹School of Pharmacy, Tongji Medical College, Huazhong University of Science and Technology, Wuhan, Hubei, China

²Department of Bioengineering and Therapeutic Sciences and Liver Center, University of California, San Francisco, CA, USA

³Key Laboratory of Carcinogenesis and Translational Research (Ministry of Education), Peking University Cancer Hospital & Institute, Beijing, China

⁴Department of Nutritional Sciences and Toxicology, UC Berkeley, Berkeley, California, USA

⁵Department of Clinical and Experimental Medicine, University of Sassari, Sassari, Italy

⁶Department of Medical Oncology, Cancer Center, State Key Laboratory of Biotherapy, West China Hospital, Sichuan University, Chengdu, China

⁷Institute of Pathology, University of Greifswald, Greifswald, Germany

⁸Department of Gastroenterology, Guizhou Provincial People's Hospital, The Affiliated People's Hospital of Guizhou Medical University, Guiyang, Guizhou Province, China

⁹Division of Gastroenterology and Hepatology, Mayo Clinic, Rochester, MN, USA

Abstract

Hepatocellular carcinoma (HCC) and intrahepatic cholangiocarcinoma (ICC) are the most prevalent types of primary liver cancer. These malignancies have limited treatment options resulting in poor patient outcomes. Metabolism reprogramming, including increased *de novo* lipogenesis, is one of the hallmarks of cancer. Fatty Acid Synthase (FASN) catalyzes the *de novo* synthesis of long-chain fatty acids from acetyl-CoA and malonyl-CoA. Increased FASN expression has been reported in multiple tumor types, and inhibition of FASN expression has been shown to have tumor-suppressing activity. Intriguingly, we found that while FASN is upregulated in human HCC samples, its expression is frequently low in human ICC specimens. Similar results

Corresponding authors: Diego F. Calvisi, Department of Clinical and Experimental Medicine, University of Sassari, via Padre Manzella 4, 07100 Sassari, Italy. Tel: 0039 079 228306; fax: 0039 079 228305; ; Email: calvisid@uniss.it; Xin Chen, UCSF, 513 Parnassus Ave., San Francisco, CA 94143, U.S.A. Tel: (415) 502-6526; ; Email: xin.chen@ucsf.edu; or Andreas Stahl, University of California, Berkeley, Berkeley, CA 94720, U.S.A. Tel: (510) 642-6900; ; Email: astahl@berkeley.edu.

*Current address: Institute of Pathology, University of Regensburg, Regensburg, Germany

Lei Li and Li Che contributed equally to the work.

Conflict of interests: nothing to disclose

were observed in mouse ICC models induced by different oncogenes. Ablating *FASN* in the mouse liver did not affect activated AKT and Notch (AKT/NICD) induced ICC formation *in vivo*. Furthermore, while both HCC and ICC lesions develop in mice following hydrodynamic injection of AKT and NRas oncogenes (AKT/Ras), deletion of *FASN* in AKT/Ras mice triggered the development almost exclusively of ICCs. In the absence of *FASN*, ICC cells might receive lipids for membrane synthesis through exogenous fatty acid uptake. In accordance with the latter hypothesis, ICC cells displayed high expression of fatty acid uptake related proteins and robust long-chain fatty acid uptake. *Conclusion*, our data demonstrate that *FASN* dependence is not a universal feature of liver tumors: while HCC development is highly dependent of *FASN* and its mediated lipogenesis, ICC tumorigenesis can be insensitive to *FASN* deprivation. Our study supports novel therapeutic approaches to treat this pernicious tumor type with the inhibition of exogenous fatty acid uptake.

Introduction

Liver cancer is among the most frequent solid tumor types and a leading cause of cancer-related death worldwide. Hepatocellular carcinoma (HCC) is the most common type of primary liver cancer.^{1,2} Treatment options for HCC are limited and generally ineffective.^{3,4} Sorafenib, a multi-kinase inhibitor and the only chemotherapeutic drug available for the treatment of unresectable HCC, has limited efficacy in improving survival of HCC patients.^{5,6} Intrahepatic cholangiocarcinoma (ICC) is the second most frequent primary liver tumor, accounting for ~10% of all liver cancers.^{7,8} ICC is an aggressive malignancy and one of the most devastating cancers of the gastrointestinal tract.⁷ The incidence and mortality rates of ICC are increasing worldwide.^{9,10} Treatment options for ICC are very limited, and there is no FDA approved targeted therapy for ICC.

Metabolic reprogramming is now recognized as one of the defining characteristics of cancer.¹¹⁻¹³ Alterations in metabolic fluxes go far beyond the well-known Warburg effect and can be observed in many sub-networks of central carbon metabolism.¹¹⁻¹³ In many cancers, aberrant fatty acid metabolism has been observed.^{14,15} In particular, it is well-established that *de novo* lipogenesis is often upregulated in solid tumors, and tumor cells become less dependent on exogenous fatty acids (FA) for growth.^{14,15} Increased expression and activity of fatty acid synthase (*FASN*), the central enzyme involved in *de novo* lipogenesis, is required for the survival and proliferation of many tumor cells and targeting *FASN* has been considered a strategy for cancer treatment.¹⁶⁻¹⁸ In our previous study, we demonstrated that *de novo* lipogenesis and *FASN* expression increase along human hepatocarcinogenesis and are inversely associated with the length of patients' survival.¹⁹ In addition, we have recently demonstrated that *FASN* depletion both suppresses AKT-driven hepatocarcinogenesis in mice and strongly restrains the growth of HCC cell lines *in vitro*.²⁰ However, whether *FASN* is also overexpressed in human ICC and required for cholangiocarcinogenesis has not been investigated to date.

In the present study, we report that, different from human HCC, expression of *FASN* is frequently downregulated in ICC tissues when compared with corresponding non-tumorous liver tissues. Similar results were obtained in various mouse ICC models. Furthermore,

ablation of *FASN* in the mouse liver did not affect AKT/NICD induced ICC formation *in vivo*. Similarly, deletion of *FASN* in AKT/Ras mice prevented development of HCC, but not ICC, leading to the predominant formation of liver tumors with cholangiocellular features. Together with the observation of robust uptake of exogenous FA by ICC, the present results suggest that upregulation of *de novo* fatty acid synthesis with concomitant decline of exogenous fatty acid uptake is not a universal feature of cancer.

Materials and Methods

Human cholangiocarcinoma samples

A collection of formalin-fixed, paraffin-embedded ICC (n=45) samples was used in the present study. Thirty frozen ICC and corresponding non-tumorous surrounding livers from the same collection were also used. The clinicopathological features of liver cancer patients are summarized in Supplementary Table 1. ICC specimens were collected in the University of Greifswald (Greifswald, Germany). Institutional Review Board approval was obtained at the local Ethical Committee of the University Medicine of Greifswald.

Constructs

The plasmids used in the study, including pT3-EF1 α -myr-AKT, pT3-EF1 α -NICD1, pT2-Caggs-NRasV12, pT3-EF1 α -Cre, pT3-EF1 α -miR-29 and pCMV-SB have been described previously.^{21–23} Angptl4/pBabe was purchased from Addgene (Plasmid #19156) and Angptl4 cDNA was cloned into pT3-EF1 α vector via Gateway cloning strategy. All plasmids were purified using the Endotoxin-free Maxi Prep Kit before injecting into mice.

Hydrodynamic injection and mouse monitoring

FASN^{fl/fl} mice in C57BL/6 background were described previously.^{24,25} *CD36*^{-/-} mice in C57BL/6 background were used as previously described.²⁶ *AlbCre* mice in C57BL/6 background²⁷ were obtained from the Jackson Laboratory (Bar Harbor, ME). *FASN*^{fl/fl} mice were crossed with *AlbCre* mice to eventually generate liver specific *FASN* knockout mice, *AlbCre*;*FASN*^{fl/fl} line. Male and female mice were used in the study, and no difference was noticed when using either male or female mice. Hydrodynamic transfection was performed as described.²⁸ Mice were housed, fed, and monitored in accordance with protocols approved by the Committee for Animal Research at the University of California, San Francisco.

Histopathologic Analysis

Liver histopathologic analysis on mouse lesions was performed by two experienced liver pathologists (ME and FD) on tissue slides stained with H&E and the PAS reaction in accordance with the criteria by Frith et al.²⁹

Detailed description of Materials and Methods is provided as Supplementary Material.

Results

Downregulation of FASN expression in human and mouse ICC samples

First, we determined the expression of FASN in human ICC samples. FASN mRNA level was analyzed in 30 paired human non-tumor liver tissue and ICC specimens using real-time quantitative RT-PCR. We found that FASN mRNA expression is significantly downregulated in ICC samples compared to respective non-tumor liver samples ($p=0.002$; Fig. 1A). Same result was obtained using TCGA microarray data of 36 surgically resected ICCs and 59 surrounding non-tumor liver tissues ($p=1 \times 10^{-7}$; Sup. Fig. 1). To further validate these findings, we examined the protein expression of FASN and its upstream inducer, Acetyl-CoA Carboxylase (ACAC), in our collection of human ICC specimens. In accordance with mRNA data, we found that FASN and ACAC immunolabeling was significantly lower in 38 and 34 of 45 ICC samples, respectively (84.4% and 75.5%, respectively), when compared with non-tumorous surrounding counterparts, as detected by immunohistochemistry (Fig. 1C, upper panel). Equivalent levels of FASN and ACAC immunoreactivity in ICC and corresponding non-neoplastic livers were detected in the remaining samples (Fig. 1C, lower panel). An equivalent trend was observed when analyzing part of the ICC collection ($n=22$) by Western blotting (Fig. 1B), where 19 of 22 samples (86.4%) showed lower levels of FASN in ICC when compared with non-neoplastic livers. Thus, our results indicate that FASN (and ACAC) is almost ubiquitously downregulated in human ICC.

We have shown the coordinated activation of AKT/mTOR and Notch cascades in human ICC specimens.²¹ In accordance with the latter findings in human ICC, hydrodynamic transfection of activated forms of AKT (myr-AKT1) and Notch1 (Notch intracellular domain 1 or NICD1) drives rapid ICC development (AKT/NICD) in mice.²¹ Thus, we determined whether FASN expression levels in liver lesions from AKT/NICD mice were altered. Consistent with the human ICC data, FASN was expressed at a much lower level in AKT/NICD cholangiocellular tumors than in surrounding non-neoplastic liver tissues (Fig. 2A). Furthermore, these lesions did not accumulate neutral-lipid droplets (as revealed by Oil Red O [ORO] staining) (Sup. Fig. 2). These results are in striking contrast with the remarkable lipogenic phenotype, elevated FASN expression, and extensive ORO-positive labeling that characterize hepatocellular lesions developed in AKT mice (Sup. Fig. 2).¹⁹

Recently, we established a murine ICC model by directly targeting biliary epithelial cells with activated AKT (myr-AKT) and Yap (YapS127A) oncogenes. In this model, ICC development requires the administration of IL33 (AKT/Yap/IL33).³⁰ Similar to AKT/NICD lesions, ICCs developed in AKT/Yap/IL33 mice exhibited downregulation of FASN when compared to non-tumorous livers (Fig. 2B).

Next, we examined FASN expression in mouse ICC induced by deletion of Pten and TP53 via CRISPR-mediated gene editing (sgPten/sgP53).³¹ Once again, we found that FASN protein is expressed at lower levels in ICCs than surrounding liver tissues from sgPten/sgP53 mice (Fig. 2C).

Finally, we investigated the levels of FASN in a mouse model characterized by the overexpression of activated forms of AKT and NRas (NRas-V12) in the liver (AKT/Ras). In

these mice, both HCC and ICC develop, with pure ICC lesions accounting for approximately 10% of the tumors.³² Preneoplastic and neoplastic hepatocellular lesions expressed high levels of FASN (Fig. 3) while cholangiocellular lesions exhibited low expression of FASN (Fig. 3), confirming our previous findings.

Altogether, the present data indicate that FASN expression is downregulated in human and mouse ICC when compared with the non-tumorous liver.

FASN is dispensable for AKT/NICD induced ICC formation in mice

Next, we investigated the functional role of FASN in cholangiocarcinogenesis. For this purpose, we determined whether FASN and *de novo* lipogenesis are required for AKT/NICD induced ICC formation taking advantage of *FASN*^{fl/fl} mice.^{24,25}

Two methods were employed to delete *FASN* in the context of overexpressing AKT and NICD oncogenes in the mouse liver (Fig. 4A). In the first approach, we hydrodynamically injected AKT/NICD together with Cre (AKT/NICD/Cre) into *FASN*^{fl/fl} mice (Fig. 4A). This method allowed us to specifically delete *FASN* while simultaneously expressing AKT and NICD1 oncogenes in the same hepatocyte population of *FASN*^{fl/fl} mice. The effectiveness of this co-injection approach has been validated in our previous publication.²² As a control, we injected AKT/NICD with a pT3EF1 α empty vector (AKT/NICD/pT3) into *FASN*^{fl/fl} mice. Of note, all AKT/NICD/Cre as well as all AKT/NICD/pT3 injected *FASN*^{fl/fl} mice became moribund and were required to be euthanized by 5 weeks post injection. No statistical difference in the survival rate between the two cohorts was detected ($p=0.59$). Multiple cystic lesions were present throughout the livers of AKT/NICD/Cre and AKT/NICD/pT3 mice (Fig. 4B). Microscopically, numerous cystoadenocarcinomas and ICC, identical to those previously detected in FVB/N mice co-injected with AKT and NICD oncogenes,²¹ occupied most of the liver parenchyma in the two mouse groups (Fig. 4C). Subsequent immunohistochemical analysis demonstrated that cholangiocellular tumors were positive for the transfected oncogenes, namely HA-tagged AKT (Fig. 4D) and Myc-tagged NICD1 (not shown), while being negative for FASN expression (Fig. 4D).

In the second approach, we generated liver specific *FASN*^{fl/fl} null mice by breeding *AlbCre* mice with *FASN*^{fl/fl} mice to eventually create *AlbCre;FASN*^{fl/fl} mice (Fig. 5). AKT/NICD oncogenes were hydrodynamically injected into *AlbCre;FASN*^{fl/fl} mice as well as control *FASN*^{fl/fl} mice (Fig. 5A). Similar to that described previously, all AKT/NICD injected *AlbCre;FASN*^{fl/fl} and *FASN*^{fl/fl} mice developed lethal burden of ICC around 5 weeks post injection and were required to be euthanized (Fig. 5B and C). No statistical difference in the survival rate between the two cohorts was found ($p=0.16$). Importantly, immunostaining demonstrated the lack of FASN expression in normal and tumor liver tissues from *AlbCre;FASN*^{fl/fl} mice (not shown). This was further validated using Western blotting (Fig. 5D), showing the expression of ectopically injected HA-tagged AKT in the tumor samples. In addition, FASN was strongly expressed in liver tumor tissues from *FASN*^{fl/fl} mice, but its expression was very low in tumors from *AlbCre;FASN*^{fl/fl} mice (Fig. 5D). The faint band of FASN protein in *AlbCre;FASN*^{fl/fl} mouse livers is likely the result of FASN expression in other cell types, such as endothelial cells.

Altogether, the present results indicate that FASN and its mediated *de novo* lipogenesis are not required for ICC development driven by AKT and NICD oncogenes.

FASN expression is required for AKT/Ras driven HCC but not ICC formation in mice

Since AKT/Ras co-expression induces the development of both HCC and ICC in the mouse liver,³² we investigated whether FASN is required for AKT/Ras driven hepatocarcinogenesis. For this purpose, we hydrodynamically injected AKT/Ras together with Cre (AKT/Ras/Cre) into *FASN^{fl/fl}* mice (Fig. 6A). AKT/Ras plasmids were co-injected with pT3 into *FASN^{fl/fl}* mice as control (AKT/Ras/pT3). All AKT/Ras/pT3 mice developed lethal burden of liver tumors by 7 to 9 weeks post injection, in accordance with our previous findings (Fig. 6B).³⁶ In contrast, AKT/Ras/Cre mice developed a high burden of liver tumors ~10 weeks post injection, and virtually all mice succumbed to liver tumors 14 weeks post injection (Fig. 6B). Histologically, liver tumors from AKT/Ras/pT3 mice appeared to be similar to those detected when AKT/Ras were injected into FVB/N wild-type mice,³² with over 80% of tumor lesions consisting of pure HCC and the remaining lesions consisting of pure ICC or mixed HCC/ICC. Indeed, sporadic CK19-positive ICC lesions could be found in AKT/Ras/pT3 liver tissues (Fig. 6C, left panel). Intriguingly, AKT/Ras/Cre mice showed a striking difference in the HCC/ICC ratio, with over 90% of the lesions being pure ICC, and very few (less than 5%) consisting of pure HCC (Fig. 6C, right panel).

Thus, FASN loss significantly affects HCC formation, but not ICC development, in AKT/Ras driven hepatocarcinogenesis.

Fatty acid uptake in mouse ICC lesions

Our data demonstrate that ICC lesions induced by AKT/NICD or AKT/Ras do not fully depend on *de novo* lipogenesis for their growth. As fatty acids (FA) are fundamentally required for tumor cell proliferation to provide new phospholipids for plasma membranes,^{14–16,18,33} the lack of FASN dependence suggests an increased role for the uptake of exogenous FA. As a first step to investigate this possibility, we analyzed the expression of the major FA transporters via endocytosis mechanisms as well as of lipoprotein lipase (LPL) and CD36 in AKT/NICD tumor cells. LPL is the enzyme responsible for extracellular lipolysis of triglycerides into FA, which are then intracellularly translocated via CD36³⁴ and/or FA transporters of the SLC27 family (FATPs).³⁵ We found that three members of the FATP family, namely SLC27A1, SLC27A2, and SLC27A5 as well as LPL and CD36 were expressed in AKT/NICD cells (Fig. 7A). In particular, while SLC27A2 and SLC27A5 were downregulated in AKT/NICD ICC compared to surrounding non-tumorous liver, SLC27A1, LPL, and CD36 were upregulated in ICC (Fig. 7A). In addition, mRNA levels of SLC27A2, SLC27A5, and CD36 were found to be downregulated in human ICC samples from the TCGA dataset, whereas SLC27A1 and LPL levels were higher in ICC samples than non-tumorous liver tissues in the same dataset (Sup. Fig. 3). Upregulation of LPL and downregulation of CD36, respectively, in human ICC when compared with corresponding non-tumorous surrounding livers was further validated in our sample collection by real-time RT-PCR (Sup. Fig. 4).

Next, we isolated normal hepatocytes as well as primary murine ICC cells from AKT/NICD injected mice and compared their FA uptake activity using a FACS based assay. Noticeably, we found that AKT/NICD tumor cells took up a fluorescent fatty acid analog (C1-Bodipy-C12) at a comparable rate to normal hepatocytes (Fig. 7B), which are known to have robust transporter mediated uptake.^{37,38} Furthermore, the HUCCT1 human ICC cell line also displayed robust uptake of exogenous FA, which was inhibited by the polyphenol phloretin, indicating a transporter mediated process³⁸ (Fig. 7C).

Thus, the present data suggest that AKT/NICD tumor cells might utilize FA released by extracellular lipolysis and/or endocytosis in a transporter-dependent manner.

AKT/NICD tumors are resistant to CD36 deprivation

Finally, we assessed if the CD36/LPL axis is the major FA uptake route required for AKT/NICD-dependent cholangiocarcinogenesis. Being that efficient utilization by cancer cells of FA released by extracellular lipolysis requires the activity of both LPL and CD36, we determined whether the deprivation of *CD36* affects AKT/NICD-driven liver carcinogenesis. For this purpose, we hydrodynamically transfected AKT/NICD oncogenes into *CD36* knockout mice³⁹ (referred to as AKT/NICD/CD36KO mice; Fig. 8). Surprisingly, we found that cholangiocarcinogenesis was neither inhibited nor delayed in AKT/NICD/CD36KO mice when compared with wild-type mice injected with AKT/NICD (AKT/NICD mice). Indeed, similar to AKT/NICD mice, AKT/NICD/CD36KO mice developed multiple ICC and were required to be euthanized 5 weeks post injection (Fig. 8). Histologically, the lesions developed in AKT/NICD/CD36KO mice consisted of ICC (Fig. 8) and they were undistinguishable to that described in AKT/NICD (Fig. 2), AKT/NICD/pT3 (Fig. 4), and AKT/NICD/Cre mice (Fig. 4). Furthermore, we inhibited LPL activity via co-injection of AKT/NICD with Angptl4 (AKT/NICD/Angptl4) or miR-29 (AKT/NICD/miR29) (Sup. Fig. 5A). Angptl4 is a well-known inhibitor of LPL,⁴⁰ whereas miR-29 inhibits LPL expression in the liver.⁴¹ We found that, comparing with control AKT/NICD/pT3 injected mice, co-injection of Angptl4 or miR29 slightly delayed the development of ICC (Sup. Fig. 5A). Nevertheless, by 6 to 7 weeks post injection, all mice developed lethal burden of liver tumor and were required to be euthanized. Histologically, the lesions developed in AKT/NICD/Angptl4 or AKT/NICD/miR29 mice consisted of ICC, similar to ICCs induced by AKT/NICD/pT3 (Sup. Fig. 5B).

Altogether, the present data indicate that disruption of the LPL/CD36 axis does not significantly affect AKT/NICD-driven cholangiocarcinogenesis.

Discussion

A significant amount of evidence indicates that metabolic alterations such as aberrant glucose, glutamine, and lipid metabolism are indicative of cancer. The Warburg effect, which refers to the fact that tumor cells rely on aerobic glycolysis instead of oxidative phosphorylation for survival, is perhaps the most studied cancer metabolic phenotype.⁴² Aberrant *de novo* FA biosynthesis is another important feature of malignant transformation.¹⁶ Most normal human tissues use dietary (exogenous) lipids for synthesis of new structural lipids, while *de novo* FA synthesis is generally suppressed. Consequently,

enzymes involved in lipogenesis, including FASN, ACAC, or stearoyl-CoA desaturase 1 (SCD1), are expressed at negligible levels in normal cells.⁴³ In contrast, in highly proliferating cancer cells, the exacerbated lipogenesis is reflected by the increased activity and expression of these lipogenic enzymes.¹⁶ FASN is the key lipogenic enzyme as it catalyzes the synthesis of palmitate from acetyl-CoA and malonyl-CoA.¹⁶ Upregulation of FASN has been reported in multiple tumor types, including breast, prostate, and renal cancer as well as in HCC.^{16,18} Inhibition of FASN via either small molecules (C75, Orlistat) or siRNA can efficiently suppress tumor cell growth *in vitro* and xenograft models.^{16,18} Importantly, a recent study showed that transgenic expression of FASN in mice results in prostate intraepithelial neoplasia,⁴⁴ supporting a direct oncogenic role of FASN and lipogenesis in prostate carcinogenesis. In the liver, although overexpression of FASN via hydrodynamic injection did not trigger tumor development, FASN suppression completely abolished AKT-dependent hepatocarcinogenesis.²⁰ In addition, strong growth restraint and massive apoptosis followed FASN silencing in HCC cell lines.¹⁹ Altogether, the present data seem to underline a crucial role of FASN in carcinogenesis and the dependence of tumors on FASN activity to grow and progress.

In human ICC, a rising and highly aggressive primary tumor of the liver,^{7,9,10} the role of FASN has not been investigated to date. In the current study, we show that in both human and mouse ICC, FASN expression is downregulated when compared with non-tumorous surrounding liver tissues. In addition, the consequent functional analyses demonstrated that FASN expression is dispensable for AKT/NICD driven cholangiocarcinogenesis in mice. Thus, the present data highlight the tissue type specific metabolic needs along carcinogenesis. The different requirement of FASN for HCC and ICC is well exemplified by AKT/Ras mice, which are characterized by the development of both HCC and ICC lesions.³² In these mice, indeed, we found that while FASN deprivation led to inhibition of HCC development, ICC normally formed, further confirming the need of FASN for hepatocarcinogenesis but not cholangiocarcinogenesis.

Given the irreplaceable role of FA for tumor cell proliferation, the decreased reliance of ICC cells on *de novo* FA synthesis implies a pivotal role for the uptake of exogenous FA. Indeed, we found that growing the HUCCT1 human ICC cell line in lipoprotein deficient media strongly inhibited cell growth (Sup. Fig. 6A). Consistently, we found that both HepG2 (a HCC cell line) and HUCCT1 exhibit comparable FA uptake in culture (Sup. Fig. 6B). The importance of the protein mediated FA uptake in HUCCT1 cells was further validated by treating cells with Phloretin (Fig. 7C). Clearly, additional FA uptake experiments using primary human HCC and ICC cells are necessary to determine the importance of this phenomenon along human hepatocarcinogenesis.

In accordance with the hypothesis that exogenous FA uptake is required for ICC tumor growth, we found that LPL, CD36, and SLC27A1 were upregulated in AKT/NICD lesions (Fig. 7A). Importantly, functional uptake studies showed that ICC derived cells were fully competent in FA uptake assays compared to hepatocytes (Fig. 7B), further supporting our hypothesis that ICC cells mainly rely on exogenous rather than newly-synthesized FA to fuel their growth. In an intriguing study, it has been recently demonstrated that selected breast and prostate cancer and liposarcoma cell lines possess an active LPL/CD36 system, whose

activity promotes cell proliferation and/or resistance to cytotoxic effects induced by FA inhibition of the same cells.⁴⁵ In addition, elevated expression of LPL and CD36 was detected in the majority of breast, liposarcoma, and prostate tumor tissues, thus suggesting a crucial role played by lipolysis of exogenous/dietary FA in cancer cells *in vivo*.⁴⁵ Following this pioneering study, we determined whether the same applies to mouse ICC. However, our data suggest that FA uptake occurs via a mechanism independent of CD36, as AKT/NICD driven cholangiocarcinogenesis is not affected by CD36 loss (Fig. 8). Consistently, suppression of LPL via miR-29 or Angptl4 has rather limited effects on AKT/NICD driven cholangiocarcinogenesis (Sup. Fig. 5). However, as human ICC display upregulation of LPL, further studies are needed to better understand the relevance of the LPL/CD36 axis in the human disease.

Another candidate that might explain the resistance of ICC cells to FASN deprivation is the FA transporter SLC27A1. Expression array analysis demonstrated that SLC27A1 expression is upregulated in human ICC samples (Sup. Fig. 3). This observation was validated by qRT real-time PCR analysis (Sup. Fig. 7). Furthermore, in a pilot study, we found that suppression of SLC27A1 by specific siRNA decreases the *in vitro* growth of the HUCCT1 and HuH28 ICC cell lines (Sup. Fig. 8, 9). Even more importantly, suppression of SLC27A1 synergized with FASN silencing to induce growth restraint of HUCCT1 and HuH28 cells (Sup. Fig. 8, 9). Clearly, additional investigations are necessary to clarify the role of SLC27A1 in cholangiocarcinogenesis.

Beside the insights on the metabolic requirements of ICC cells, the present findings might have important clinical implications. Indeed, although FASN inhibitors have shown promising anti-neoplastic effects in many experimental tumor models, the same drugs might be ineffective against ICC, at least when used alone. Of note, it has been shown that FA uptake is an inherently druggable process and inhibitors have been described for SLC27A1.⁴⁶ Based on the preliminary data from the present study, it is conceivable that inhibitors of FA uptake, either alone or in association with FASN inhibitors, might be beneficial for the treatment of human ICC.

Supplementary Material

Refer to Web version on PubMed Central for supplementary material.

Acknowledgments

We are grateful to Dr. Wen Xue (Massachusetts Institute of Technology, Cambridge, MA) for providing sgPten/sgP53 mouse ICC blocks; and to Dr. Clay F. Semenkovich (Washington University, St. Louis, MO) for providing *FASN^{fl/fl}* mice.

Financial support: This work was supported by grant from the Italian Association Against Cancer (AIRC; grant number IG 12139) to DFC; NIH R01CA136606 to XC; R21CA187306 to XC and AS; and P30DK026743 for UCSF Liver Center; and National Natural Science Foundation of China (Grant No. 81201553) to Lei Li.

List of Abbreviations

ACAC acetyl-CoA carboxylase

AKT	v-akt murine thymoma viral oncogene homolog
FA	fatty acids
FASN	fatty acid synthase
HCC	hepatocellular carcinoma
ICC	intrahepatic cholangiocarcinoma
LPL	lipoprotein lipase
NICD	Notch intracellular domain 1
N-Ras	neuroblastoma Ras viral oncogene homolog
siRNA	small interfering RNA

References

1. El-Serag HB. Epidemiology of viral hepatitis and hepatocellular carcinoma. *Gastroenterology*. 2012; 142:1264–1273. e1261. [PubMed: 22537432]
2. Mittal S, El-Serag HB. Epidemiology of hepatocellular carcinoma: consider the population. *J Clin Gastroenterol*. 2013; 47(Suppl):S2–6. [PubMed: 23632345]
3. Villanueva A, Llovet JM. Liver cancer in 2013: Mutational landscape of HCC--the end of the beginning. *Nat Rev Clin Oncol*. 2014; 11:73–74. [PubMed: 24395088]
4. Villanueva A, Llovet JM. Targeted therapies for hepatocellular carcinoma. *Gastroenterology*. 2011; 140:1410–1426. [PubMed: 21406195]
5. Llovet JM, Ricci S, Mazzaferro V, Hilgard P, Gane E, Blanc JF, de Oliveira AC, et al. Sorafenib in advanced hepatocellular carcinoma. *N Engl J Med*. 2008; 359:378–390. [PubMed: 18650514]
6. Kane RC, Farrell AT, Madabushi R, Booth B, Chattopadhyay S, Sridhara R, Justice R, et al. Sorafenib for the treatment of unresectable hepatocellular carcinoma. *Oncologist*. 2009; 14:95–100. [PubMed: 19144678]
7. Razumilava N, Gores GJ. Cholangiocarcinoma. *Lancet*. 2014; 383:2168–2179. [PubMed: 24581682]
8. Rizvi S, Borad MJ, Patel T, Gores GJ. Cholangiocarcinoma: molecular pathways and therapeutic opportunities. *Semin Liver Dis*. 2014; 34:456–464. [PubMed: 25369307]
9. Gatto M, Bragazzi MC, Semeraro R, Napoli C, Gentile R, Torrice A, Gaudio E, et al. Cholangiocarcinoma: update and future perspectives. *Dig Liver Dis*. 2010; 42:253–260. [PubMed: 20097142]
10. Pinter M, Hucke F, Zielonke N, Waldhor T, Trauner M, Peck-Radosavljevic M, Sieghart W. Incidence and mortality trends for biliary tract cancers in Austria. *Liver Int*. 2014; 34:1102–1108. [PubMed: 24119058]
11. Ward PS, Thompson CB. Metabolic reprogramming: a cancer hallmark even warburg did not anticipate. *Cancer Cell*. 2012; 21:297–308. [PubMed: 22439925]
12. Cantor JR, Sabatini DM. Cancer cell metabolism: one hallmark, many faces. *Cancer Discov*. 2012; 2:881–898. [PubMed: 23009760]
13. Schulze A, Harris AL. How cancer metabolism is tuned for proliferation and vulnerable to disruption. *Nature*. 2012; 491:364–373. [PubMed: 23151579]
14. Santos CR, Schulze A. Lipid metabolism in cancer. *Febs J*. 2012; 279:2610–2623. [PubMed: 22621751]
15. Currie E, Schulze A, Zechner R, Walther TC, Farese RV Jr. Cellular fatty acid metabolism and cancer. *Cell Metab*. 2013; 18:153–161. [PubMed: 23791484]
16. Menendez JA, Lupu R. Fatty acid synthase and the lipogenic phenotype in cancer pathogenesis. *Nat Rev Cancer*. 2007; 7:763–777. [PubMed: 17882277]

17. Mullen GE, Yet L. Progress in the development of fatty acid synthase inhibitors as anticancer targets. *Bioorg Med Chem Lett*. 2015; 25:4363–4369. [PubMed: 26364942]
18. Flavin R, Peluso S, Nguyen PL, Loda M. Fatty acid synthase as a potential therapeutic target in cancer. *Future Oncol*. 2010; 6:551–562. [PubMed: 20373869]
19. Calvisi DF, Wang C, Ho C, Ladu S, Lee SA, Mattu S, Destefanis G, et al. Increased lipogenesis, induced by AKT-mTORC1-RPS6 signaling, promotes development of human hepatocellular carcinoma. *Gastroenterology*. 2011; 140:1071–1083. [PubMed: 21147110]
20. Li L, Pilo GM, Li X, Cigliano A, Latte G, Che L, Joseph C, et al. Inactivation of fatty acid synthase impairs hepatocarcinogenesis driven by AKT in mice and humans. *J Hepatol*. 2015; 64:333–341. [PubMed: 26476289]
21. Fan B, Malato Y, Calvisi DF, Naqvi S, Razumilava N, Ribback S, Gores GJ, et al. Cholangiocarcinomas can originate from hepatocytes in mice. *J Clin Invest*. 2012; 122:2911–2915. [PubMed: 22797301]
22. Wang C, Cigliano A, Jiang L, Li X, Fan B, Pilo MG, Liu Y, et al. 4EBP1/eIF4E and p70S6K/RPS6 axes play critical and distinct roles in hepatocarcinogenesis driven by AKT and N-Ras proto-oncogenes in mice. *Hepatology*. 2015; 61:200–213. [PubMed: 25145583]
23. Tao J, Ji J, Li X, Ding N, Wu H, Liu Y, Wang XW, et al. Distinct anti-oncogenic effect of various microRNAs in different mouse models of liver cancer. *Oncotarget*. 2015; 6:6977–6988. [PubMed: 25762642]
24. Chakravarthy MV, Pan Z, Zhu Y, Tordjman K, Schneider JG, Coleman T, Turk J, et al. “New” hepatic fat activates PPARalpha to maintain glucose, lipid, and cholesterol homeostasis. *Cell Metab*. 2005; 1:309–322. [PubMed: 16054078]
25. Chakravarthy MV, Zhu Y, Lopez M, Yin L, Wozniak DF, Coleman T, Hu Z, et al. Brain fatty acid synthase activates PPARalpha to maintain energy homeostasis. *J Clin Invest*. 2007; 117:2539–2552. [PubMed: 17694178]
26. Anderson CM, Kazantzis M, Wang J, Venkatraman S, Goncalves RL, Quinlan CL, Ng R, et al. Dependence of brown adipose tissue function on CD36-mediated coenzyme Q uptake. *Cell Rep*. 2015; 10:505–515. [PubMed: 25620701]
27. Postic C, Shiota M, Niswender KD, Jetton TL, Chen Y, Moates JM, Shelton KD, et al. Dual roles for glucokinase in glucose homeostasis as determined by liver and pancreatic beta cell-specific gene knock-outs using Cre recombinase. *J Biol Chem*. 1999; 274:305–315. [PubMed: 9867845]
28. Chen X, Calvisi DF. Hydrodynamic transfection for generation of novel mouse models for liver cancer research. *Am J Pathol*. 2014; 184:912–923. [PubMed: 24480331]
29. Frith CH, Ward JM, Turusov VS. Tumours of the liver. *IARC Sci Publ*. 1994:223–269. [PubMed: 8082908]
30. Yamada D, Rizvi S, Razumilava N, Bronk SF, Davila JJ, Champion MD, Borad MJ, et al. IL-33 facilitates oncogene-induced cholangiocarcinoma in mice by an interleukin-6-sensitive mechanism. *Hepatology*. 2015; 61:1627–1642. [PubMed: 25580681]
31. Xue W, Chen S, Yin H, Tammela T, Papagiannakopoulos T, Joshi NS, Cai W, et al. CRISPR-mediated direct mutation of cancer genes in the mouse liver. *Nature*. 2014; 514:380–384. [PubMed: 25119044]
32. Ho C, Wang C, Mattu S, Destefanis G, Ladu S, Delogu S, Armbruster J, et al. AKT (v-akt murine thymoma viral oncogene homolog 1) and N-Ras (neuroblastoma ras viral oncogene homolog) coactivation in the mouse liver promotes rapid carcinogenesis by way of mTOR (mammalian target of rapamycin complex 1), FOXM1 (forkhead box M1)/SKP2, and c-Myc pathways. *Hepatology*. 2012; 55:833–845. [PubMed: 21993994]
33. Swinnen JV, Brusselmans K, Verhoeven G. Increased lipogenesis in cancer cells: new players, novel targets. *Curr Opin Clin Nutr Metab Care*. 2006; 9:358–365. [PubMed: 16778563]
34. Wang H, Eckel RH. Lipoprotein lipase: from gene to obesity. *Am J Physiol Endocrinol Metab*. 2009; 297:E271–288. [PubMed: 19318514]
35. Anderson CM, Stahl A. SLC27 fatty acid transport proteins. *Mol Aspects Med*. 2013; 34:516–528. [PubMed: 23506886]

36. Andersen JB, Spee B, Blechacz BR, Avital I, Komuta M, Barbour A, Conner EA, et al. Genomic and genetic characterization of cholangiocarcinoma identifies therapeutic targets for tyrosine kinase inhibitors. *Gastroenterology*. 2012; 142:1021–1031. e1015. [PubMed: 22178589]
37. Doege H, Grimm D, Falcon A, Tsang B, Storm TA, Xu H, Ortegon AM, et al. Silencing of hepatic fatty acid transporter protein 5 in vivo reverses diet-induced non-alcoholic fatty liver disease and improves hyperglycemia. *J Biol Chem*. 2008; 283:22186–22192. [PubMed: 18524776]
38. Falcon A, Doege H, Fluit A, Tsang B, Watson N, Kay MA, Stahl A. FATP2 is a hepatic fatty acid transporter and peroxisomal very long-chain acyl-CoA synthetase. *Am J Physiol Endocrinol Metab*. 2010
39. Febbraio M, Abumrad NA, Hajjar DP, Sharma K, Cheng W, Pearce SF, Silverstein RL. A null mutation in murine CD36 reveals an important role in fatty acid and lipoprotein metabolism. *J Biol Chem*. 1999; 274:19055–19062. [PubMed: 10383407]
40. Dijk W, Kersten S. Regulation of lipoprotein lipase by Angptl4. *Trends Endocrinol Metab*. 2014; 25:146–155. [PubMed: 24397894]
41. Mattis AN, Song G, Hitchner K, Kim RY, Lee AY, Sharma AD, Malato Y, et al. A screen in mice uncovers repression of lipoprotein lipase by microRNA-29a as a mechanism for lipid distribution away from the liver. *Hepatology*. 2015; 61:141–152. [PubMed: 25131933]
42. Vander Heiden MG, Cantley LC, Thompson CB. Understanding the Warburg effect: the metabolic requirements of cell proliferation. *Science*. 2009; 324:1029–1033. [PubMed: 19460998]
43. Weiss L, Hoffmann GE, Schreiber R, Andres H, Fuchs E, Korber E, Kolb HJ. Fatty-acid biosynthesis in man, a pathway of minor importance. Purification, optimal assay conditions, and organ distribution of fatty-acid synthase. *Biol Chem Hoppe Seyler*. 1986; 367:905–912. [PubMed: 3790257]
44. Migita T, Ruiz S, Fornari A, Fiorentino M, Priolo C, Zadra G, Inazuka F, et al. Fatty acid synthase: a metabolic enzyme and candidate oncogene in prostate cancer. *J Natl Cancer Inst*. 2009; 101:519–532. [PubMed: 19318631]
45. Kuemmerle NB, Rysman E, Lombardo PS, Flanagan AJ, Lipe BC, Wells WA, Pettus JR, et al. Lipoprotein lipase links dietary fat to solid tumor cell proliferation. *Mol Cancer Ther*. 2011; 10:427–436. [PubMed: 21282354]
46. Matsufuji T, Ikeda M, Naito A, Hirouchi M, Kanda S, Izumi M, Harada J, et al. Arylpiperazines as fatty acid transport protein 1 (FATP1) inhibitors with improved potency and pharmacokinetic properties. *Bioorg Med Chem Lett*. 2013; 23:2560–2565. [PubMed: 23528296]

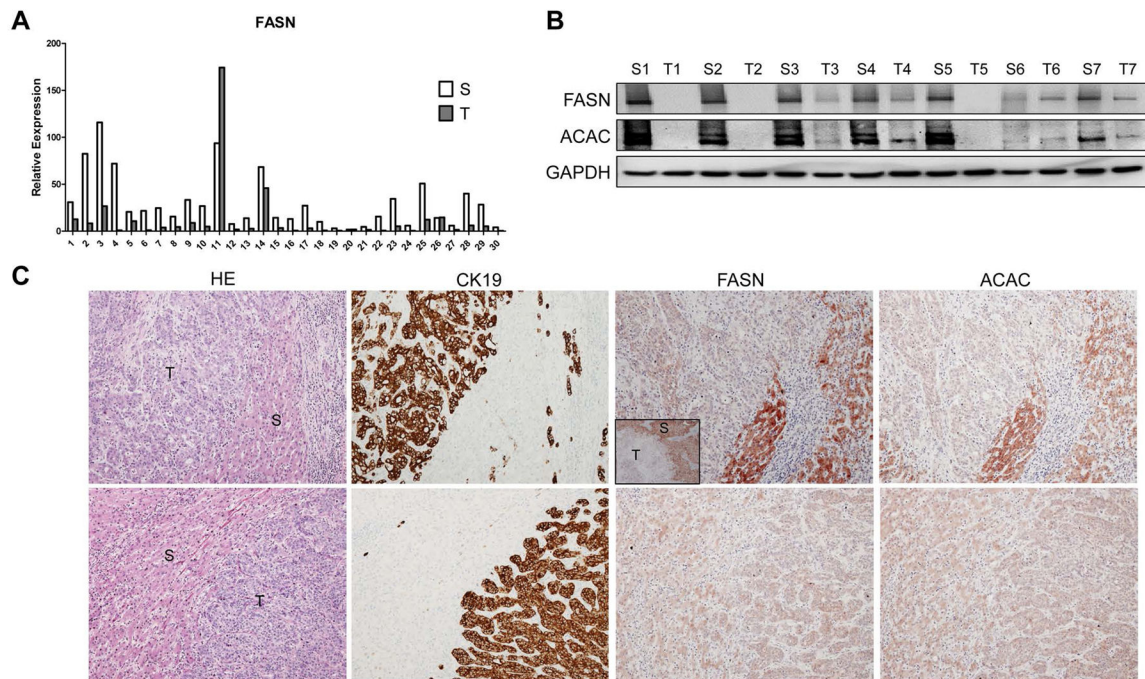


Figure 1. Expression of FASN in human ICC samples. (A) qRT-PCR analysis of FASN mRNA expression in 30 paired human ICC (T) and non-tumor surrounding liver tissues (S); (B) Representative Western blot analysis of paired non-tumorous surrounding livers (S) and ICC (T) showing the downregulation of FASN and its upstream inducer, ACAC, in human ICC. GAPDH was used as a loading control. (C) Immunohistochemical patterns of FASN and ACAC in human ICC specimens. Upper panel, ICC (T) showing downregulation of FASN and ACAC when compared to the non-neoplastic counterpart (S). Lower panel, equivalent immunoreactivity for FASN protein in an ICC and surrounding non-tumorous liver. CK19 was used as a cholangiocellular marker. Original magnification: 40X in inset; 100X in all the other pictures. Abbreviation: HE, hematoxylin and eosin staining.

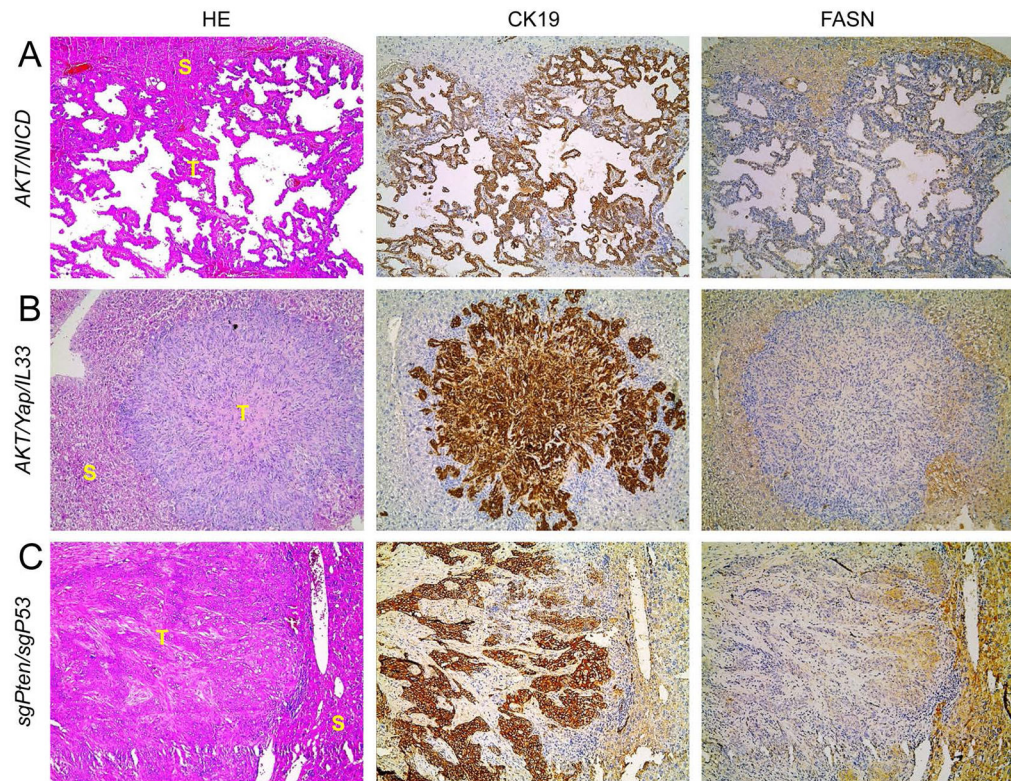


Figure 2.

FASN expression pattern in AKT/NICD, AKT/Yap/IL33, and sgPten/sgP53 mouse models, as detected by immunohistochemistry. Similar to human ICC specimens, immunoreactivity for FASN is either faint or absent in ICC (T), whereas it is preserved in non-tumorous surrounding liver (S). Original magnification: 100X. Abbreviation: HE, hematoxylin and eosin staining. At least 3 mice in each tumor group were analyzed by immunostaining.

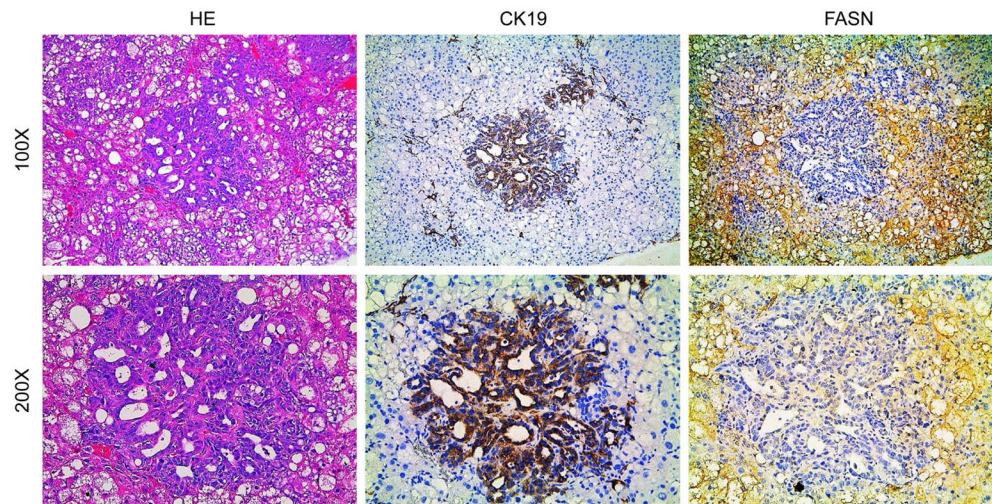


Figure 3. FASN expression patterns in cholangiocellular lesions from AKT/Ras mice, as detected by immunohistochemistry. Upper panel, immunoreactivity for FASN is low in CK19(+) cholangiocellular lesions, whereas lipid-rich preneoplastic and neoplastic lesions exhibit strong immunoreactivity for FASN. Lower panel, details of the pictures shown in the upper panel. Original magnification: 100X in the upper panel; 200X in the lower panel. Abbreviation: HE, hematoxylin and eosin staining. Liver tumor samples from 5 AKT/Ras injected mice were analyzed by immunostaining.

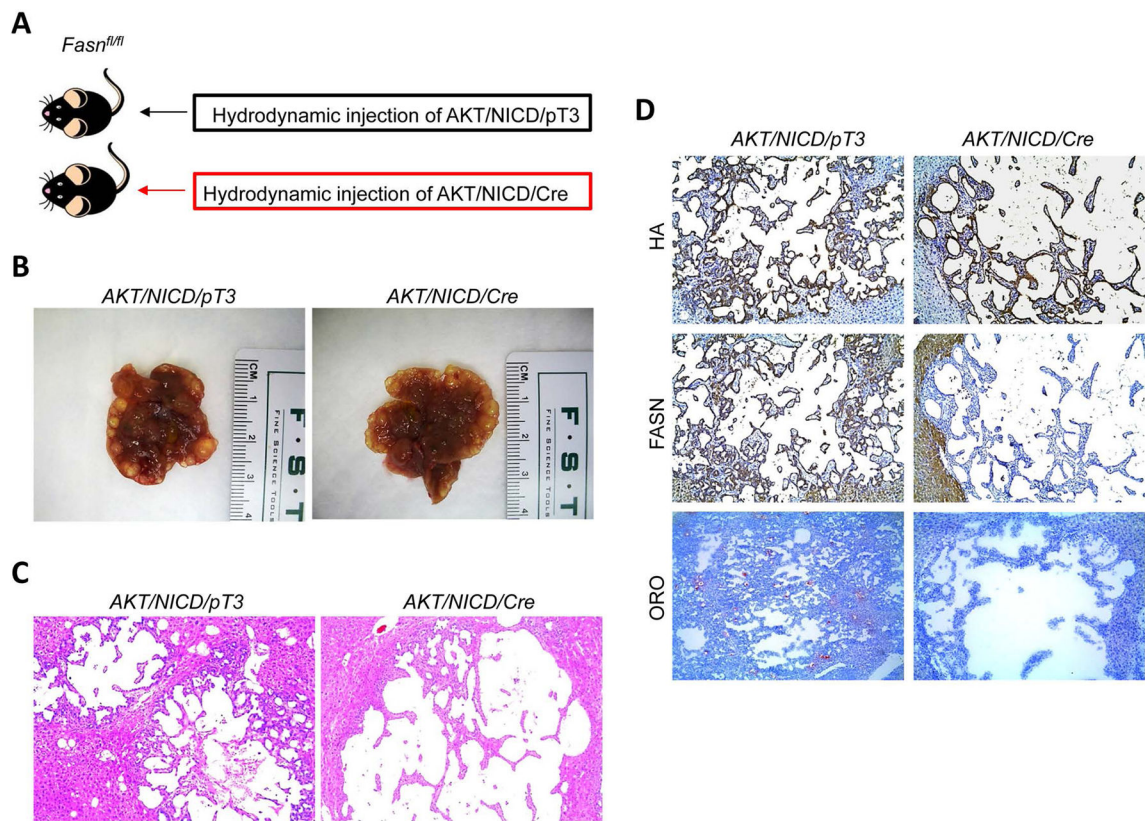


Figure 4.

AKT/NICD induced ICC development does not require FASN. (A) Scheme of the hydrodynamic gene delivery strategy: activated forms of AKT and NICD were hydrodynamically injected together with Cre into *FASN^{fl/fl}* mice (AKT/NICD/Cre, n=5). This method allows the deletion of *FASN* while simultaneously expressing AKT and NICD1 in the same *FASN^{fl/fl}* hepatocytes. As control, AKT and NICD were injected in the same mice together with the empty vector (AKT/NICD/pT3, n=5). (B) Macroscopically, livers from AKT/NICD/Cre and AKT/NICD/pT3 mice exhibited the presence of multiple cysts. (C) Microscopically, cysts consisted of ICC that were indistinguishable in the two mouse groups. (D) Immunohistochemical and histochemical patterns for HA-tagged AKT, FASN, and lipid storage (as revealed by Oil-redO or ORO staining) in AKT/NICD/Cre and AKT/NICD/pT3 mice. While immunolabeling for HA-Tag was equivalent in the two mouse groups, staining for both FASN and ORO was lost in AKT/NICD/Cre lesions and preserved in AKT/NICD/pT3 lesions. Original magnification: 40X. Abbreviation: HE, hematoxylin and eosin staining.

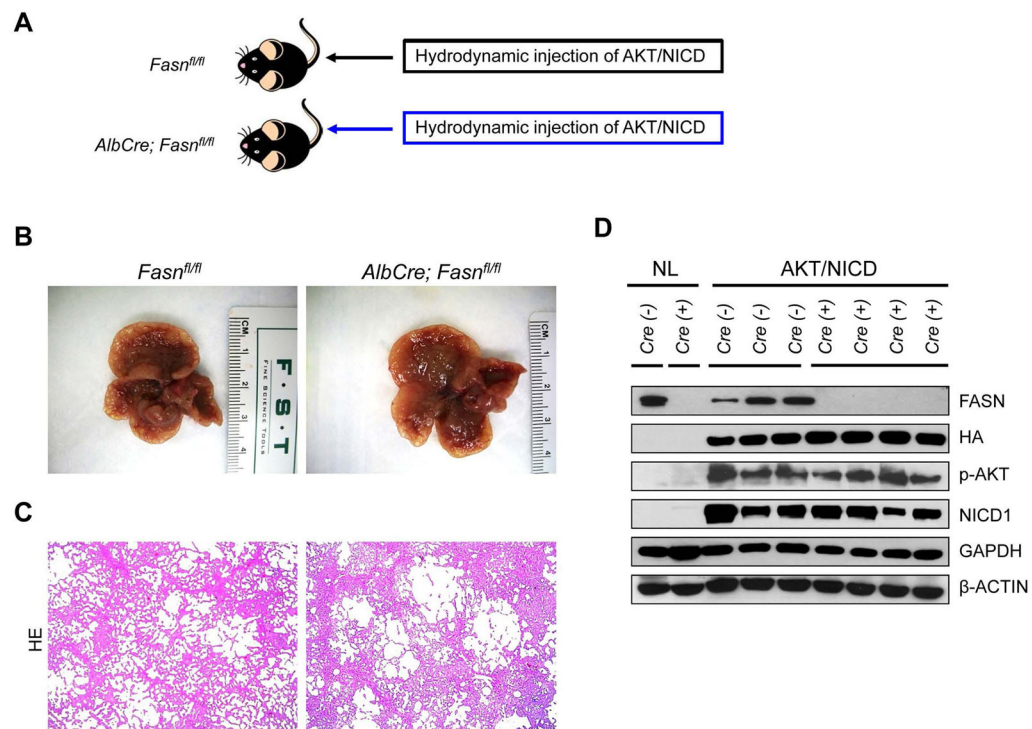


Figure 5.

Genetic ablation of *FASN* in the mouse liver does not affect tumor development driven by AKT/NICD co-expression. (A) Study design. Overexpression of AKT/NICD promotes the development of multiple cholangiocellular tumors both in *FASN*^{fl/fl} mice with an intact *FASN* gene (*FASN*^{fl/fl} mice, n=5) and those where *FASN* was deleted by the Cre system (*AlbCre*;*FASN*^{fl/fl} mice, n=6). (B) Livers from both mouse groups showed the presence of numerous cysts. (C) Microscopically, cysts consisted of ICC that were undistinguishable in *FASN*^{fl/fl} and *AlbCre*;*FASN*^{fl/fl} mice. (D) Western blot analysis in normal livers (NL) from *FASN*^{fl/fl} (Cre⁻) and *AlbCre*;*FASN*^{fl/fl} mice (Cre⁺) mice, and ICC lesions from AKT/NICD injected *FASN*^{fl/fl} (Cre⁻) and *AlbCre*;*FASN*^{fl/fl} mice (Cre⁺) mice. In the latter group, the levels of *FASN* are extremely low due to Cre-mediated deletion. Original magnification: 40X. Abbreviation: HE, hematoxylin and eosin staining.

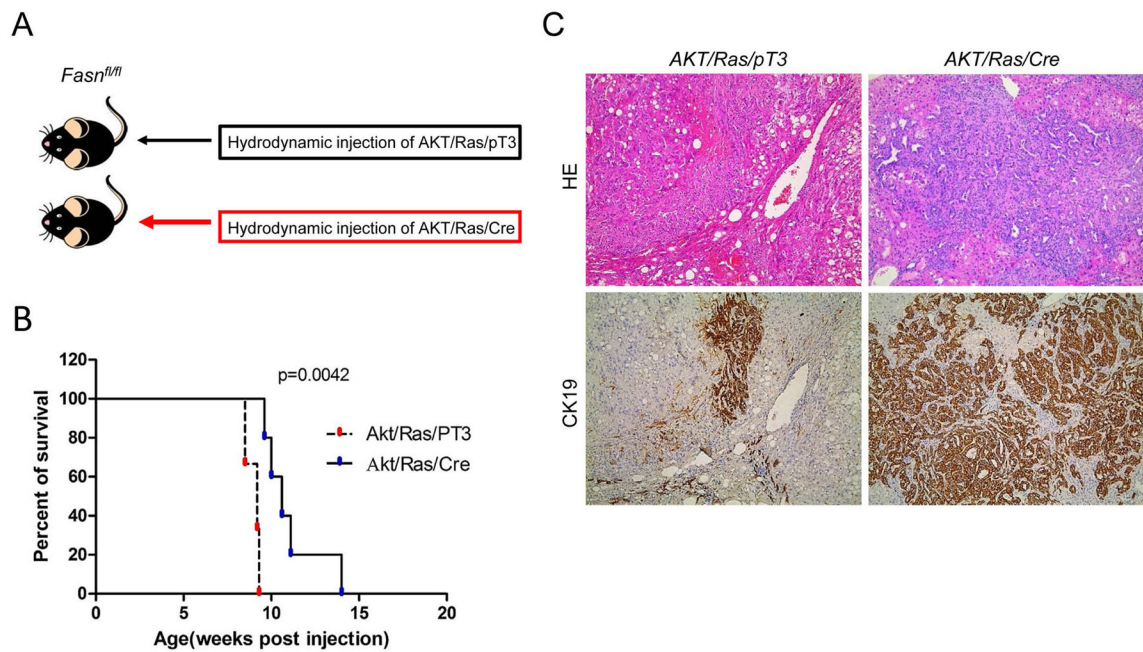


Figure 6.

Inhibition of HCC but not ICC development in *FASN^{fl/fl}* mice injected with activated forms of AKT and Ras. (A) Study design: activated forms of AKT and NRas (N-RasV12) were hydrodynamically injected together with Cre into *FASN^{fl/fl}* mice (AKT/Ras/Cre). As control, AKT and NRasV12 were injected in the same mice together with the empty vector (AKT/Ras/pT3). (B) Survival curve of AKT/Ras/Cre (n=5) and AKT/Ras/pT3 mice (n=5). (C) Microscopically, AKT/Ras/pT3 livers consisted mostly of lipid-rich, hepatocellular lesions with few CK19(+) cholangiocellular lesions. In striking contrast, deletion of FASN by the Cre system resulted in the almost complete disappearance of hepatocellular lesions but the expansion of cholangiocellular CK(+) lesions in AKT/Ras/Cre mice. Original magnification: 40X. Abbreviation: HE, hematoxylin and eosin staining.

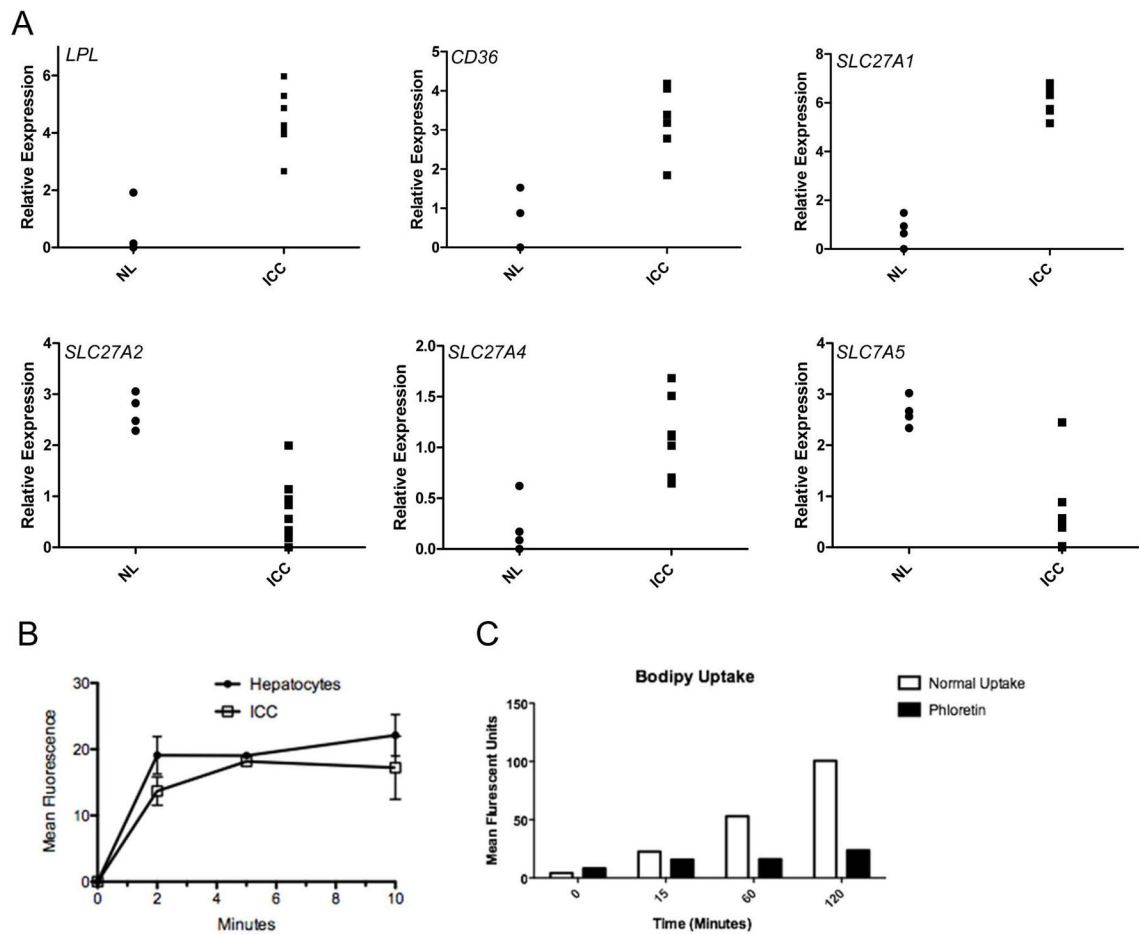


Figure 7. Expression of fatty acid transporters in human and mouse ICC cells. (A) Expression of CD36, LPL, SLC27A1, SLC27A2 and SLC27A5 in AKT/NICD tumor tissues (ICC) versus normal mouse liver tissues (NL). (B) Fatty acid uptake measured with a fluorescent fatty acid analogue, BODIPY® 500/510 C₁, C₁₂ (4,4-Difluoro-5-Methyl-4-Bora-3a,4a-Diaza-*s*-Indacene-3-Dodecanoic Acid), in primary cell suspension from AKT/NICD ICC cells as well as normal mouse hepatocytes. (C) Uptake of fluorescent fatty acid analogue in HUCCT1 cells with or without phloretin, β -(4-Hydroxyphenyl)-2,4,6-trihydroxypropiophenone, an inhibitor of active transport.

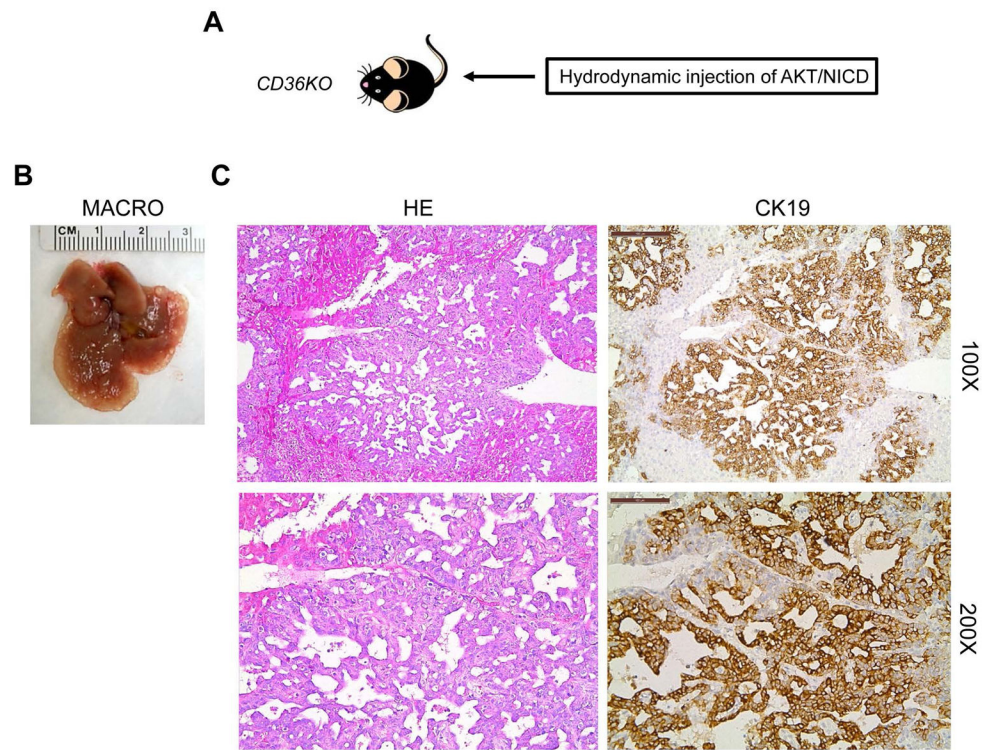


Figure 8. Ablation of *CD36* does not affect AKT/NICD driven cholangiocarcinogenesis. (A) Study design: activated forms of AKT and NICD1 were hydrodynamically injected into *CD36* knockout (*CD36KO*) mice (n=5). (B) Macroscopically (macro), livers from AKT/NICD injected *CD36KO* mice showed the presence of multiple cysts. (C) Microscopically, cysts consisted of ICC that were indistinguishable from those developed in AKT/NICD injected wild-type mice. Original magnification: 100X in upper panels; 200X in lower panels. Abbreviation: HE, hematoxylin and eosin staining.